Available online at www.sciencedirect.com
ScienceDirect
Quaternary Research 68 (2007) 18–27
QUATERNARY RESEARCH
www.elsevier.com/locate/yqres

Annual precipitation in the Yellowstone National Park region since AD 1173

Stephen T. Gray [a,*], Lisa J. Graumlich [b], Julio L. Betancourt [c]

[a] *Water Resources Data System and Office of the Wyoming State Climatologist, University of Wyoming, Laramie WY 82071, USA*
[b] *Big Sky Institute, Montana State University, Bozeman, MT 59717, USA*
[c] *Desert Laboratory, U.S. Geological Survey, Tucson, AZ 85745, USA*

Received 9 October 2006
Available online 12 April 2007

Abstract

Cores and cross sections from 133 limber pine (*Pinus flexilis* James) and Douglas fir (*Pseudotsuga menziesii* (Mirbel) Franco) at four sites were used to estimate annual (July to June) precipitation in the Yellowstone National Park region for the period from AD 1173 to 1998. Examination of the long-term record shows that the early 20th century was markedly wet compared to the previous 700 yr. Extreme wet and dry years within the instrumental period fall within the range of past variability, and the magnitude of the worst-case droughts of the 20th century (AD 1930s and 1950s) was likely equaled or exceeded on numerous occasions before AD 1900. Spectral analysis showed significant decadal to multidecadal precipitation variability. At times this lower frequency variability produces strong regime-like behavior in regional precipitation, with the potential for rapid, high-amplitude switching between predominately wet and predominately dry conditions. Over multiple time scales, strong Yellowstone region precipitation anomalies were almost always associated with spatially extensive events spanning various combinations of the central and southern U.S. Rockies, the northern U.S.–Southern Canadian Rockies and the Pacific Northwest.

Keywords: Drought; Paleoclimate; Tree rings; Decadal to multidecadal variability; Greater Yellowstone Region; Rocky Mountains

Introduction

Concerns over anthropogenic climate change, as well as recent multiyear droughts that taxed supplies of water and other natural resources, emphasize the importance of understanding natural climatic variability in the Rocky Mountain West. The hydroclimate of Yellowstone National Park (YNP; Fig. 1) is of particular interest given the area's conservation value and its role as headwaters for both the Columbia and Missouri rivers. The impact of pre-instrumental climate in shaping YNP landscapes is also hotly debated (Romme et al., 1995; NRC (National Research Council), 2002; Larsen and Ripple, 2003), and the outcome of these debates will undoubtedly impact how the park is managed for future climatic variability and change.

In light of this pressing need, there has been a surprising lack of high-resolution proxy reconstructions of YNP regional climate. Romme et al. (1995) used tree rings to infer patterns of past moisture variability in the region, but this work was based on a single chronology and did not employ rigorous dendroclimatological calibration and verification methods. Graumlich et al. (2003) offer a statistically verified tree ring reconstruction of Yellowstone River flow for the period AD 1706 through 1999. However, this work was geared toward understanding Pacific Basin controls on regional climate, and the resulting proxy record may not be appropriate for some applications in land management and ecosystem science. Gridded reconstructions of the June–August Palmer Drought Severity Index are now available for all of the conterminous United States (e.g., Cook et al., 2004), but these records may not adequately capture vital winter precipitation variability in the YNP region.

Here we present a new tree-ring-based reconstruction of annual (July–June) YNP precipitation spanning AD 1173–1998. The reconstruction is based on a set of four tree ring chronologies from sites within and adjacent to YNP (Fig. 1b). We use this long record to examine interannual variations within the instrumental period and prior to the AD 1890s. We then employ spectral analysis and related methods to investigate possible decadal to multidecadal variability in YNP precipitation. Finally, using

* Corresponding author. Fax: +1 307 766 3785.
E-mail address: stateclim@wrds.uwyo.edu (S.T. Gray).

0033-5894/$ - see front matter © 2007 University of Washington. All rights reserved.
doi:10.1016/j.yqres.2007.02.002

information from existing paleoclimate proxies, we explore how variability in YNP precipitation relates to extensive drought/wet events across western North America.

Methods

Yellowstone region tree ring chronologies

Samples were taken at four sites in the mountains and foothills surrounding YNP (Fig. 1b). Yellow Mountain Ridge (YMR) is located in the southern Madison Range near Big Sky, Montana. The Mount Everts (MEV) site is near Mammoth, Wyoming, approximately 10 km south of the park boundary. Both Carter Mountain (CM) and Wood River Canyon (WRC) are located in the Absaroka mountains to the southeast of YNP. At three of the four sites (i.e., YMR, CM and WRC), we sampled limber pine (*Pinus flexilis*; Table 1). Douglas fir (*Pseudotsuga menziesii*) were sampled at MEV. At least two increment cores were taken from each living tree that was sampled, and cores or sections were taken from available dead wood. All sampling was performed in open stands growing on shallow or rocky soils. In addition to samples collected in 1999–2001, the final MEV chronology incorporates series collected by C.W. Fergusson and D.G. Despain during the early 1970s. In combination, these four sites provide 183 samples taken from 133 trees.

After mounting and sanding, the cores and sections were cross dated using standard methods. Ring widths in each sample were measured to the nearest 0.001 mm, and cross dating was verified using the COFECHA program (Holmes, 1983). We used the negative exponential curve or linear regression (horizontal line or line with negative slope) functions in the ARSTAN program (Cook, 1985) to remove age-related growth trends from individual series. Series were then combined into site chronologies using a bi-weight robust mean function. We produced two versions of each chronology. The first version is a

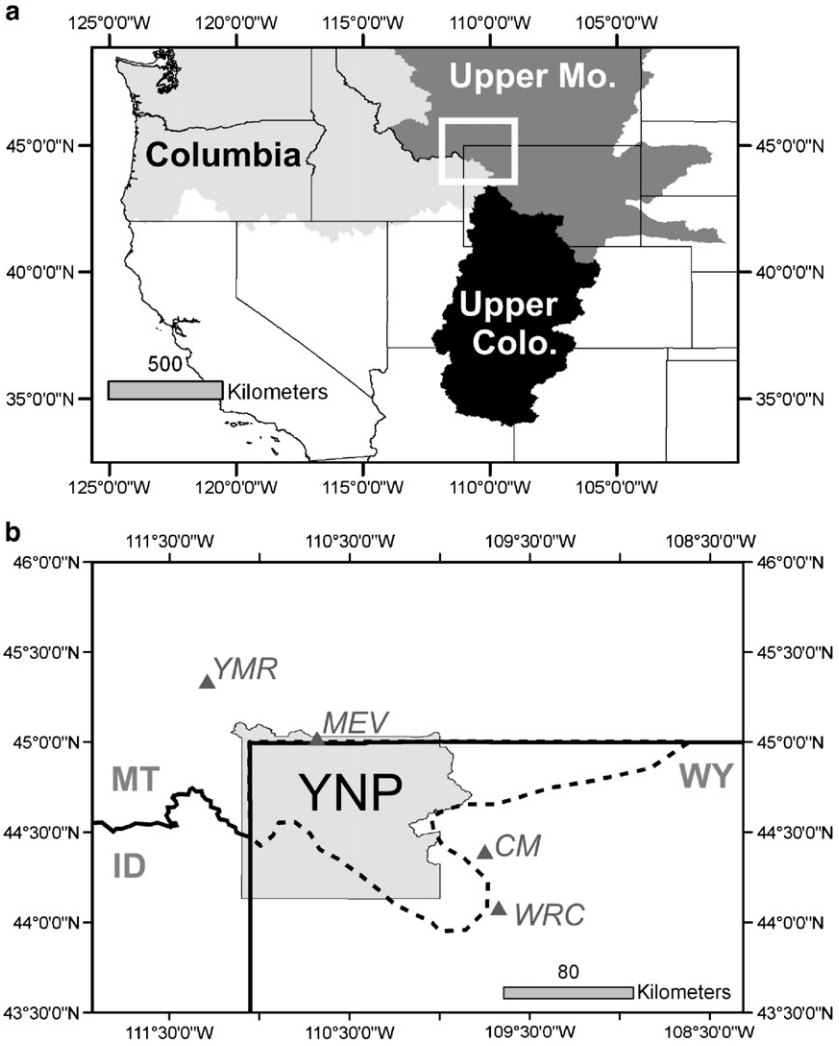

Figure 1. (a) Map of western North America showing the location of Yellowstone National Park (YNP) and surrounding hydroclimatic regions discussed in the this study. (b) Detail of the Greater Yellowstone Region study area (from white box in panel a), including the boundary of Yellowstone National Park and Wyoming Climate Division 1 (dashed line). The locations of tree ring sites used in this study are shown as triangles. Sites names are coded as follows: CM = Carter Mountain; MEV = Mount Everts; WRC = Wood River Canyon; YMR = Yellow Mountain Ridge.

Table 1
Descriptive statistics for the individual site chronologies used in the reconstruction

Chronology[a]	Species	Elevation (m)	Time span (yr AD)	Year SSS >0.85	Number of trees	Number of series (radii)	Average series length (yr)	Inter-series correlation (%)
Carter Mountain[b]	*P. flexilis*	2400–2600	1062–2000	1254	20	28	451.0	0.73
Mount Everts[c]	*P. menziesii*	2100–2200	1173–1999	1243	43	65	288.3	0.59
Wood River Canyon[b]	*P. flexilis*	2200–2600	1105–2000	1258	21	27	460.5	0.68
Yellow Mountain Ridge[d]	*P. flexilis*	2400–2500	1172–1998	473	49	63	341.3	0.25

[a] All chronologies are archived and available for download via the International Tree Ring Data Bank (http://www.ncdc.noaa.gov/paleo/treering.html).
[b] Contributed by S. Gray, S. Jackson and J. Betancourt.
[c] Contributed by L. Graumlich, L. Waggoner, J. King and E. Fergusson.
[d] Contributed by J. King, L. Waggoner and L. Graumlich.

prewhitened or residual chronology where any significant low-order persistence has been removed, and the resulting records have autocorrelations at a lag of 1 yr between −0.04 (WRC) and 0.01 (CM). The second version is a standard chronology where low-order persistence has been retained. In the standard chronologies, autocorrelation at a lag of 1 yr ranged between 0.47 (CM) and 0.57 (WRC).

Testing climate–growth linkages

In order to examine the link between ring widths and climate at these sites, we compared measures of Yellowstone regional temperature and precipitation for the current year (t), previous year ($t-1$) and following year ($t+1$) against both standard and residual chronology values. More specifically, correlation values with bootstrapped confidence intervals (Biondi and Waikul, 2005) were calculated for monthly, seasonal (e.g., JJA, DJF, NDJFM, etc.) and 12-month precipitation and temperature from state climate divisions surrounding Yellowstone NP (Fig. 1). All divisional data were obtained from the National Climatic Data Center (http://lwf.ncdc.noaa.gov/oa/climate/climatedata.html) and cover the period from AD 1895 to present.

Residual ring width chronologies at all sites showed significant relationships with Wyoming Division 1 precipitation over some part of the year, and examples of these correlations are shown in Table 2. MEV shows a winter-dominated signal (January $r=0.40$), while ring growth at CM and WRC is more tightly linked to summer moisture (June $r=0.35$ and 0.34, respectively). YMR displays a mixed seasonal precipitation signal (July $r=0.25$; January $r=-0.22$). Total annual precipitation for the water year (October–September) and July–June were well correlated with ring width chronologies at all sites. Twelve-month precipitation was positively correlated with chronologies from the MEV, CM and WRC sites ($r=0.25$ to 0.66; $p<0.05$), but negatively correlated ($r=-0.21$ to -0.26; $p<0.05$) with YMR. All site chronologies were significantly correlated with measures of growing season temperature. On the whole, temperature–growth relationships were weaker than those between precipitation and growth. The one exception is YMR, our northernmost and most snow-dominated site.

Results from the correlation analyses were similar using standard chronologies (not shown). Comparable correlations were seen with records from Montana Climate Divisions 2 and 5, as well as Wyoming Climate Divisions 2 and 4, but relationships were generally highest with Wyoming Division 1. Individual station records from the Yellowstone region were also examined. However, correlations between these stations and the chronologies were generally lower than for divisional data. Though generally weaker than climate–growth correlations in more arid regions like the southwestern United States, the values observed here are comparable to those from surrounding regions (Gray et al., 2004a; Pederson et al., 2005).

Table 2
Representative correlations between Greater Yellowstone Region (Wyoming Climate Division 1) climate records and tree growth at the Yellow Mountain Ridge (YMR), Mount Evert (MEV), Carter Mountain (CM) and Wood River Canyon (WRC) sites

Variable	YMR	MEV	CM	WRC
January PCP	−0.22	0.40	0.25	NS
June PCP	NS	0.21	0.35	0.34
July PCP	0.25	0.19*	NS	NS
November–March PPT	−0.26	0.38	NS	NS
October–September PPT	−0.25	0.38 *	0.38 *	0.24*
July–June PPT	−0.21	0.66	0.32	0.25
June–August TMP	0.29	−0.42	−0.20	−0.19

All correlations shown are significant at $p<0.05$ or better as determined from bootstrapped confidence intervals (Biondi and Waikul, 2005). PCP = precipitation; TMP = temperature.
* Highest correlations were seen at $t-1$.

The climate–growth model

Based on the correlation analyses, we chose two potential metrics for reconstruction: total October–September precipitation and total July–June precipitation. In both cases, forward stepwise regression was used to calibrate tree growth against observed precipitation. Potential predictors consisting of current year and 1-yr lagged residual chronology values were entered into the model in order of their variance explained. The threshold for entry of a predictor was set to a p-value of ≤ 0.05, with $p<0.10$ required for retention. We evaluated the strength of the resulting models based on adjusted r^2, F-values and the PRESS statistic (Weisberg, 1985). Potential multicollinearity of predictors was examined using the variance inflation factor (VIF; Haan, 2002), and autocorrelation of residuals was assessed on the basis of residual plots and the Durbin–Watson statistic (Weisberg, 1985). In order to avoid over-fitting, the

Table 3
Statistics for observed and reconstructed annual (July–June) precipitation values

	F-value	*r*	r^2	Adjusted r^2
(a) Regression results				
Observed vs. reconstructed values (1896–1998)	28.00**	0.73**	0.54**	0.52**
Sign test (agree/disagree)	RE[a]	PRESS	Durbin–Watson[b]	Mallows' Cp[c]
(b) Verification results				
73/29*	0.52	277.3	1.59	5.5
Series	Mean	SD	Skew	*r*(1)[d]
(c) Descriptive statistics				
Observed (1896–1998)	398	58.9	0.14	0.28
Reconstructed (1896–1998)	399	43.3	0.07	0.06
Reconstructed (1258–1998)	397	46.7	−0.15	0.05
Reconstructed (1173–1998)	396	47.3	−0.08	0.07

[a] Reduction of error (RE) statistic; positive value indicates that the regression model is a better predictor of precipitation than the mean for the observed values (Fritts, 1976).
[b] Indicates no significant autocorrelation of residuals (Weisberg, 1985).
[c] Indicates that the model is relatively precise (has small variance) in estimating the true regression coefficients and predicting responses outside the calibration data set (Draper and Smith, 1998).
[d] Autoregression at a lag of 1 yr.
* Significant at $p<0.01$.
** Significant at $p<0.001$.

stepwise process was terminated when root mean squared error (RMSE; Weisberg, 1985) showed an increase between steps.

The stepwise analysis produced a three-variable model in three steps for October–September precipitation having adjusted $r^2=0.33$ ($p<0.001$, Table 3). However, a four-predictor model for July–June precipitation (four steps) showed an adjusted $r^2=0.52$ ($p<0.001$). This model incorporates values from each of the four site chronologies:

Total July–June precipitation = 9.50 – 3.77 YMR + 4.87 MEV + 3.85 CM + 1.17 WRC_{t-1}.

The *F*-value and PRESS statistic were also more favorable for the July–June model than for October–September (28.6 vs. 14.3 and 277.3 vs. 529.3, respectively). Plots of residuals (not shown) and the Durbin–Watson statistic (1.58) did not indicate any potential problems with residual autocorrelation in the July–June model (Table 3). All VIFs for the July–June model were close to one, suggesting that there were was no significant multicollinearity among the predictors (Haan, 2002).

The magnitude of several wet years in the AD 1940s and early 1950s, as well as some dry years such as 1933 and 1961, is not well estimated by the July–June model (Fig. 2a). However, the July–June model captures the sign of most departures (29 misses vs. 73 agreements) and the relative ranking of wet/dry years (e.g., Spearman's rank test: $r=0.70$, $p<0.001$). Multiyear trends (e.g., wetness of the 1940s, dryness of the 1930s) were also well represented by the model (Table 3). As a result, we discarded the potential October–September model and retained the July–June model for all further analyses.

Evaluating the model

We examined the stability of the July–June model using a multiple subsetting and validation approach. First the model was calibrated on half of the observed data set (e.g., 1896–1946) and then verified against the remaining values (e.g., 1947–1998). The calibration window was then shifted forward by 1 yr (e.g., 1897–1947) and the resulting model again verified against the reserved data (e.g., 1950–1998 and 1896). We evaluated model performance over the verification period on the basis of adjusted r^2 and the reduction of error statistic (RE; Fritts, 1976). This process was repeated for all possible

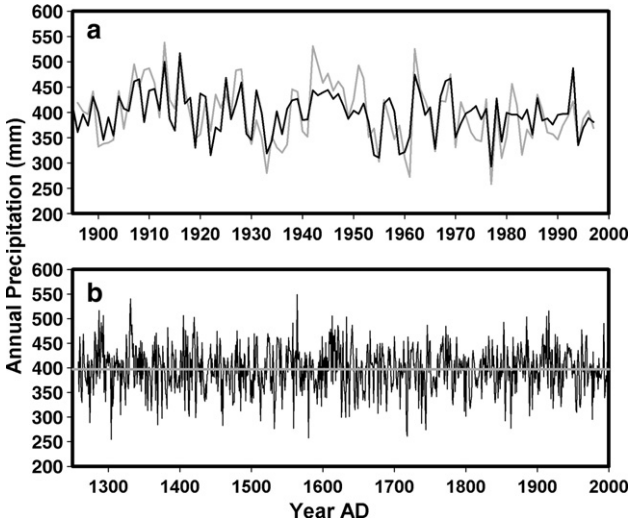

Figure 2. (a) Observed annual (previous July through current year June) precipitation for Wyoming Climate Division 1 (gray line) vs. estimates of precipitation based on the stepwise regression (black line) model. (b) The full stepwise version of reconstructed annual precipitation (black line) for AD 1173 to 1998. The horizontal line (solid gray) near 400 mm represents the series mean, and the vertical line (dotted gray) at AD 1258 divides the well-replicated portion of the record from reconstructed values in the earlier, less-replicated years (see Methods).

combinations of calibration and verification windows. Verification-period adjusted r^2 ranged from 0.41 to 0.52 ($p<0.001$), indicating that the July–June model was robust to choice of calibration period. Likewise RE values between 0.42 and 0.54 for all combinations of calibration/verification subsets suggested that the July–June model has significant predicative skill. Use of alternative regression procedures (e.g., best subsets, principal components regression) did not yield any significant model improvements.

The observed July–June precipitation series showed an autocorrelation value of 0.28 at a lag of 1 yr. Because our original model employed residual chronologies, its estimates of July–June precipitation have essentially no autocorrelation (0.06 at a lag of 1 yr). Therefore, we investigated the effect of using tree ring chronologies where low-order autocorrelation was not removed on estimates of July–June precipitation. For this analysis, the standard chronologies (autocorrelation preserved) where subjected to stepwise regression under the same rules used to create the original residual-based model. The standard chronology July–June model was similar to the residual model (same predictors, same sign for coefficients) but showed small improvements in fit (adjusted $r^2=0.54$, $F=30.44$, $p<0.001$). However, the precipitation estimates from this standard chronology model showed very high 1-yr lag autocorrelation (0.61). This large amount of persistence is likely produced by physiological lags in tree growth or other non-climatic factors (Fritts, 1976). Such levels of low-order autocorrelation may, in turn, produce spurious low-frequency signals and amplify the magnitude of multiyear droughts and wet events in the long-duration reconstruction (Woodhouse et al., 2006). The residual-based model, on the other hand, forces precipitation estimates upward (downward) following a dry (wet) year. In effect, the original model provides a more conservative estimate of past drought and wet events and an unbiased means to examine potential lower frequency (decadal and multidecadal) variations in past climate. Therefore, we judged the residual-based model to be a better choice for reconstructing values outside the instrumental period.

Finally, all four chronologies cover the period from AD 1173 to 1998, but the number of series decreases with time since present. Because of this declining sample depth, each chronology was assessed using the subsample signal strength criterion (SSS; Wigley et al., 1984). The SSS value for WRC drops below 0.85 (85% of the full chronology signal retained) in AD 1257 and below 0.85 at CM and MEV in AD 1254 and 1243, respectively. As a result, we used only the post-1257 portion of the reconstruction in the statistical analyses of past precipitation.

Spectral analysis of reconstructed Greater Yellowstone Region precipitation

In order to identify the significant modes of YNP precipitation variability, we performed a multi-taper method (MTM) analysis (Mann and Lees, 1996) on the best-replicated portion of the reconstruction (i.e. AD 1258 to 1998). MTM is an ideal method for determining the frequency characteristics of long-duration proxy records because it provides a robust means for separating the noise and signal components of a time series, particularly in data sets that may contain both periodic and quasi-periodic behavior. In addition, the use of MTM requires very few *a priori* assumptions concerning the structure of the time series. We used a 5×3 π taper and a red noise background in our analysis.

Results and discussion

Long-term precipitation variability in Yellowstone National Park

The full YNP precipitation reconstruction (Fig. 2b) shows strong interannual variability throughout the entire AD 1173 to 1998 period. In the 20th century, both the instrumental and proxy records are marked by extreme (0.05 quantile) drought years at AD 1955 and 1977 (Table 4; Figs. 2a–b). Although somewhat less severe in the tree ring estimate, a strong drought is also recorded in AD 1933. Many notable dry years occurred prior to the instrumental period. The driest years between AD 1258 and 1998, the portion of the reconstruction with the greatest sample depth, occurred in the early 14th (AD 1304) and late 16th centuries (AD 1580) when we estimate that less than 260 mm of precipitation fell in the YNP region compared to the long-term mean of 397 mm (Table 4). A remarkable pair of dry years, ranked as the 3rd and 4th driest in the proxy record, is seen at AD 1717–1718. Taken as a whole, the proxy record suggests that the worst-case drought years of the instrumental period were likely equaled or exceeded at least thirty times in the preceding six centuries.

The 20th century AD contained four of the wettest years (0.95 quantile) in the AD 1258–1998 period (Table 4; Figs. 2a–b). Two of these extremely wet years occurred during the AD 1910s (i.e. 1913 and 1916). The year AD 1962 is notable for being the 25th wettest in the well-replicated portion of the proxy record, but also

Table 4
Top fifteen driest and wettest years from the Yellowstone National Park region annual precipitation reconstruction, plus relative rankings of other extreme dry (0.05 quantile) and wet (0.95 quantile) events from the 20th century (shown in bold)

Rank	Dry year	PPT (mm)	Rank	Wet year	PPT (mm)
1	1304	255	1	1564	549
2	1580	258	2	1331	540
3	1718	261	*3*	1287	516
4	1717	274	4	**1916**	516
5	1744	274	5	1293	507
6	1532	276	6	1405	507
7	1559	277	7	1613	506
8	1863	277	8	**1913**	505
9	1460	283	9	1633	503
10	1369	284	10	1885	503
11	1738	288	11	1420	503
12	1274	289	12	1330	500
13	1513	292	13	1853	493
14	1855	293	14	1290	492
15	**1977**	295	15	1558	491
26	**1955**	309	16	**1993**	490
35	**1954**	315	25	**1962**	477

for following a severe (0.10 quantile) dry year at 1961. The wettest single year between AD 1258 and 1998 occurred in 1564, with an estimated 549 mm of precipitation (long-term mean = 397 mm). Estimated precipitation for the year AD 1216 was 544 mm, but this year falls in the less replicated portion of the reconstruction. Again, the wettest years of the instrumental period were within the range of long-term variability.

In addition to interannual fluctuations, our analysis reveals that precipitation in the YNP region varies over decadal to multidecadal time scales. The MTM spectra for the AD 1258–1998 portion of the record shows significant power centered at 14 and 20 yr (Fig. 3a). When the entire reconstruction is smoothed to highlight this lower frequency variability, decadal-scale dry periods are seen during the 1950s and at approximately 1430–1440, 1505–1520 and 1795–1825 (Fig. 3b). The early to mid 18th century AD is particularly dry, having three >10 yr drought periods that rival the magnitude of the AD 1950s event.

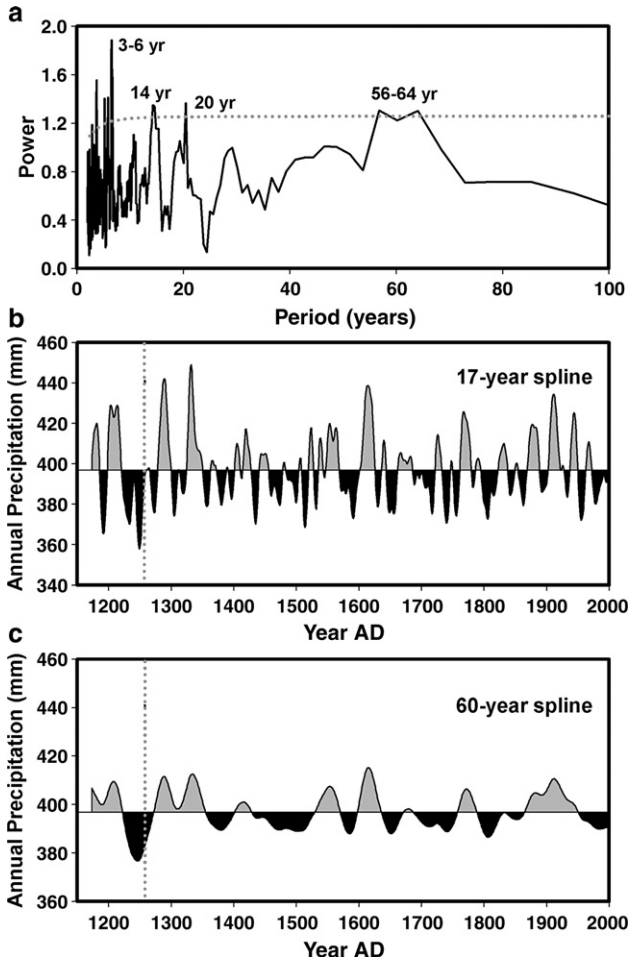

Figure 3. (a) Multi-taper method (MTM) spectrum for the reconstructed precipitation over the AD 1258–1998 period. The dotted gray line depicts the 95% significance level when compared to background red noise. (b) 17-yr and (c) 60-yr cubic smoothing splines fit to the full annual precipitation reconstruction. The thin horizontal line (solid black) near 400 mm represents the series mean, and persistent wet (gray shading) and dry (black shading) events are plotted relative to this mean. The vertical line (dotted gray) at AD 1258 divides the well-replicated portion of the record from reconstructed values in earlier years (see Methods).

The smoothed record also features numerous decadal to multidecadal wet periods. The early 20th century AD, for example, is notable for a series of decades with some of the greatest precipitation surpluses in the entire reconstruction (Fig. 3b). Following the droughts of the late 16th century AD, we see a strong wet period from roughly 1600 to 1625, and the late 13th and early 14th centuries AD are marked by several wet decades. Again, the magnitude of events in the early portions of the record (pre-AD 1258) should be viewed with caution, but the reconstruction begins with a major 20-yr wet period.

Additional significant power ($p < 0.05$) is found in a band from 56 to 64 yr (Fig. 3a). This multidecadal variability is manifest throughout the reconstruction as persistent regional precipitation anomalies (Fig. 3c). Key multidecadal precipitation events include a strong mid 13th century AD drought and a late 19th to early 20th century pluvial that persisted for ~80 yr.

Reconstructed Yellowstone precipitation in the context of other proxy records

Grid-based (2.5° × 2.5°) reconstructions of the summer (June, July and August) Palmer Drought Severity Index (PDSI) are now available for all of the western United States and parts of western Canada and Mexico (Cook et al., 2004). These PDSI reconstructions are not strictly independent of our YNP precipitation record. Some of the series included in the MEV chronology, for example, were also used by Cook et al. (2004) in PDSI reconstructions for grid cells immediately surrounding our study area. However, averaging reconstructed PDSI values over large hydroclimatic regions did allow us to examine how dry years in YNP relate to larger patterns of summer drought across western North America. More specifically PDSI values were averaged separately across the Columbia, Upper Missouri and Colorado River basins (Fig. 1a). We then compared extreme dry years (0.05 quantile) in the YNP annual precipitation reconstruction against the occurrence of different levels (0.05, 0.10 and 0.25 quantile) of summer drought in each of these regions over the period AD 1258 to 1998. In this way the potential impact of having data in the MEV chronology inform both our reconstruction and those from Cook et al. is minimized by the fact that many hundreds of additional tree ring records also contribute to each of these regional PDSI composites.

Based on these comparisons, 32 of 37 extreme dry years (0.05 quantile) in the YNP reconstruction were accompanied by summer drought (PDSI ≤ 0.25 quantile level) in one or more of the adjacent hydroclimatic regions. Over 72% of extreme YNP dry years were matched by summer droughts in the Upper Missouri, with eleven of these Upper Missouri events at the 0.05 quantile level. The coincidence of YNP dry years and summer drought was also high in comparisons with reconstructed Colorado and Columbia region PDSI (17 of 37 and 23 of 37 yr, respectively). Only three YNP dry years were accompanied by wet conditions in any of the surrounding hydroclimatic regions.

Most (32 of 37) 0.95 quantile years in the YNP reconstructions were also paired with wet summers (PDSI ≥ 0.75 quantile

level) in surrounding regions. Some 61% of YNP wet years coincided with wet summers in two or more of the adjacent hydroclimatic regions, and 31% were wet summers in all three regions. Again, we found only three instances where extreme wetness in the annual YNP record was matched with even moderate (0.25 quantile) drought in the regional PDSI records.

Comparable tree-ring-based reconstructions of annual precipitation or other proxy records that integrate both warm and cool season precipitation are not available for much of western North America. However, comparisons between our YNP record and a small set of reconstructions from surrounding regions suggest that patterns of large-scale drought/wet events seen in the PDSI records have strong analogs over multi-seasonal to annual time scales. Of the fifteen driest years in the YNP reconstruction (Table 4), twelve were also extreme drought years (0.05 quantile) in a reconstruction of annual precipitation from the Bighorn Basin (Gray et al., 2004a), the region immediately east of our study area. Likewise almost half (6 of 13) of the extreme YNP drought years over the period AD 1750–1979 were drought years (<0.25 quantile) in reconstructions of annual (October–September) precipitation for eastern Oregon (Garfin and Hughes, 1996). Comparisons with a reconstruction of Upper Colorado River flow (Woodhouse et al., 2006), a measure of regional climate integrating winter and spring precipitation, showed similar levels of simultaneous drought (12 or 22 yr). Over 90% of YNP extreme wet years (≥0.95 quantile) were also matched by wet conditions in these reconstructions.

The fact that YNP drought/wet years can be linked with similar anomalies across large portions of the Pacific Northwest, Northern Rockies and Southwest likely stems from a variable response to the El Nino-Southern Oscillation (ENSO). The southwestern United States is typically drier than average during La Niña years and wetter than average during El Niños (Cayan et al., 1999). The reverse (i.e., dry during El Niño) is generally true for the Pacific Northwest and the northern U.S. Rockies. The Yellowstone region, however, lies near a transition zone between the Southwest and Pacific Northwest response types. The strength and sign of the YNP response to an ENSO event may depend, in turn, on the magnitude of SST anomalies in the Tropical Pacific. There is also a complex response to ENSO variability within the YNP region. High-elevation snow basins and western YNP, roughly the "winter-wet" regions in the classification of Whitlock and Bartlein (1993), are likely to show a Pacific Northwest-type response, particularly during the winter months (Graumlich et al., 2003; Gray et al., 2004a). Areas where summer precipitation accounts for a larger percentage of the annual total, generally the lower elevations and sites near the eastern boundary of YNP, may sometimes favor a southwestern-type response or show no significant relation to ENSO forcing (Gray et al., 2004a).

Modes of decadal to multidecadal moisture variability similar to those in the YNP record appear in tree ring records from throughout western North America (Gray et al., 2003; Hidalgo, 2004; Pederson et al., 2005). Figure 4 compares multidecadal variability across major river basins (Columbia, Upper Missouri, Upper Colorado) adjacent to YNP. The low-frequency variability is highly synchronized across these basins at times (prior to AD 1300 and from AD 1500 to 1650), while less synchronous in others (the 1400s and post-1650). A particularly interesting period is the 13th century AD, which began with relatively wet conditions at YNP and across the three basins. General drying ensued in all basins after AD 1225, but the droughts persisted later in the Upper Missouri and Upper Colorado. For example, the driest years in the Upper Colorado were from AD 1276 to 1299 (the so-called "Great Drought" that contributed to the Anasazi abandonment of the Four Corners region; Dean, 1994), while the 1280s and 1290s were unusually wet in YNP (Figs. 3b–c and 4).

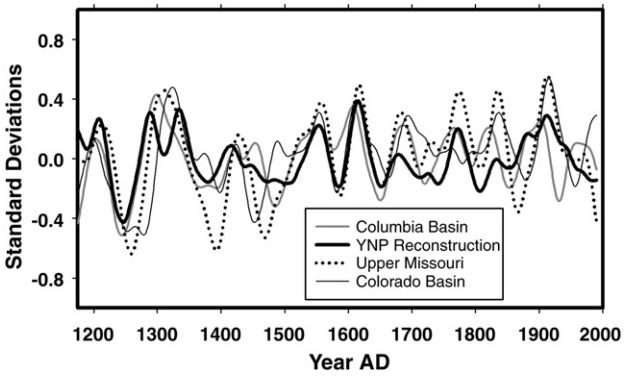

Figure 4. Comparison of 60-yr cubic smoothing splines fit to the Yellowstone regional precipitation reconstruction and 60-yr splines fit to composite drought records developed for the three large hydroclimatic basins adjoining the study area (see Fig. 1a). Series from the surrounding basins are based on the gridded PDSI reconstructions of Cook et al. (2004).

The staggered 13th century droughts occurred in the midst of a strong secular wetting trend that marked the end of the Medieval Warm Period (Cook et al., 2004). Evidence from a variety of paleoenvironmental archives suggests that the resulting march of pluvials punctuated by extreme droughts led to major changes in the structure of forests and woodlands across the Rocky Mountain Region (Swetnam and Brown, 1992; Dean, 1994; Gray et al., 2006). In particular, the wet-to-dry switch in the early 13th century AD likely favored widespread disturbances in YNP (e.g., fires, insect outbreaks, etc.). When coupled with drought-related mortality, these disturbances would have reset demographic clocks and opened niches within many woody plant communities (Swetnam and Betancourt, 1998; Gray et al., 2006). Recent studies suggest that sustained wet periods may be particularly strong drivers of ecosystem change (e.g., Brown and Wu, 2005), and pluvial conditions in the late 13th and early 14th centuries AD likely led to the recruitment of large cohorts of trees and shrubs that would dominate these landscapes for centuries to come. This phenomenon has not been specifically documented in YNP, but we suggest that the magnitude of these 13th and 14th century climatic regime shifts likely favored a major reorganization of the region's ecosystems. High-resolution studies of pollen, macrofossils and charcoal in laminated lake sediments, as well as detailed tree ring demography of woody plant communities, could further refine the relationship between these climatic events and regional ecosystem dynamics.

High-amplitude switching between decadal-scale wet and dry regimes also characterizes the late 15th through mid-17th centuries AD (Figs. 3b–c and 4). Though not as severe as some other decadal-scale droughts in the YNP record, the late 16th century AD dry period is notable for being part of the most widespread and severe droughts to affect western North America over the past 500 yr (Woodhouse and Overpeck, 1998; Stahle et al., 2000; Gray et al., 2003). As in YNP, in many areas this late 16th century AD "megadrought" was followed by a strong pluvial (Fig. 4). Again, this wet/dry combination had a major impact on ecosystems throughout western North America (Swetnam and Betancourt, 1998; Brown and Wu, 2005). The YNP wet period spanning the late 19th to early 20th centuries AD (Fig. 4) was also entrained in a series of sub-continental pluvial events (Cook et al., 2004; Gray et al., 2004a, 2006; Woodhouse et al., 2006).

The Pacific Decadal Oscillation (PDO; Mantua et al., 1997) and similar interdecadal modes in North Pacific sea surface temperatures (SSTs) account for a large portion of the lower frequency variability and resulting persistent dry/wet events in YNP over the instrumental period (Cayan et al., 1998; Dettinger et al., 1998; Graumlich et al., 2003; Gray et al., 2004a). It is also likely that the PDO modulates ENSO responses in this area (McCabe and Dettinger, 1999). However, the fact that past decadal–multidecadal precipitation regimes in YNP have been entrained in both southwestern U.S. and Pacific Northwest patterns again indicates a complex response to forcing from the Pacific Basin.

SST variations associated with the Atlantic Multidecadal Oscillation (AMO), the leading mode of lower frequency North Atlantic climate variability, contain strong signals in the 50- to 70-yr band (Enfield et al., 2001). Statistical associations have been demonstrated between western North American drought and the AMO (e.g., Enfield et al., 2001; McCabe et al., 2004). In a principal components analysis of the 20-yr drought frequencies across the United States in the 20th century, McCabe et al. (2004) showed broad spatial coherence of droughts in times of North Atlantic warming. Broadly coherent pluvials were likewise seen during North Atlantic cooling. Using actual global SST histories and isolating the influence of individual ocean basins, Sutton and Hodson (2005) were able to simulate summer drought in the Midwest and western United States with North Atlantic warming. A physical link between the AMO and winter precipitation in the western United States, however, has yet to be established. For the 20th century, both Schubert et al. (2004) and Seager et al. (2005) were able to reproduce both high- and low-frequency variability in Midwest and Southwest U.S. precipitation with climate model simulations forced with actual global SST histories. Much of this variability can be forced with tropical Pacific SSTs alone, although inclusion of SST variability in the extratropical oceans does help explain more of the variance. At multidecadal to secular time scales there is a tendency for the North Atlantic and the eastern tropical Pacific to covary in opposite phase (e.g., the Medieval Warm Period and the Little Ice Age), perhaps in response to both solar and volcanic radiative forcing (Mann et al., 2005).

Other researchers have commented on the changing synchroneity of decadal to multidecadal variability in western North American climate (Gray et al., 2003; Hidalgo, 2004; Meko and Woodhouse, 2005; Jain et al., 2005), which could be influenced by low-frequency, global SST variability. In a principal components analysis of the Cook et al. (2004) PDSI reconstructions, Hidalgo (2004) noted broad synchroneity across much of the West when the primary mode of variability was multidecadal (30–70 yr; AD 1525–1650, 1850–present), but less synchroneity when bidecadal variability (10–30 yr; AD 1700–1825) was dominant and characterized by a strong Pacific Northwest/Southwest dipole. Such strong PDO-like variability may cancel out Northwest-like vs. Southwest-like responses in the northern and southern parts of the Colorado River Basin and could explain dampened variability in Upper Colorado streamflow reconstructions from AD 1700–1850 (e.g., Woodhouse et al., 2006). In a 500-yr reconstruction of the AMO, Gray et al. (2004b) identified a prolonged period of dampened North Atlantic variability when the AMO was neutral from AD 1700 to 1850. Using the Zebiak–Cane climate model and radiative forcing, Mann et al. (2005) were able to simulate a period of dampened ENSO variability during this same period. Again, questions linger about whether AMO variability is physically modulating precipitation in the West or simply aliasing for low-frequency SST variability in the eastern tropical Pacific.

Given the importance of YNP precipitation for natural systems and human populations far beyond the park's boundaries, and the societal risks of floods or droughts spanning multiple basins simultaneously, identifying the factors that control lower frequency climate variability and synchroneity across the western United States will be a key challenge for future studies. Recent work has also shown how the impacts of decadal-scale climatic regimes can modulate the impact of human activities on large natural areas like national parks (e.g., Pederson et al., 2005). Natural regime-like behavior may alternately mask or amplify secular trends related to anthropogenic warming, thereby increasing the range of future climate scenarios (Gray et al., 2006). It is essential that natural decadal to multidecadal variability be addressed in assessments of human impacts on regional physical and biological systems, as well as in change detection and mitigation efforts.

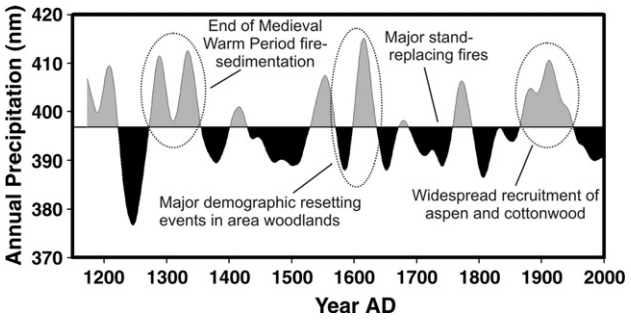

Figure 5. Major disturbance events and landscape transitions in the greater Yellowstone area (after Romme et al., 1995; Meyer and Pierce, 2003; Larsen and Ripple, 2003) related to precipitation regimes captured in this reconstruction. Precipitation data are the 60-yr smoothed series shown in Fig. 3c.

Potential applications

In addition to its potential use in understanding regional climate variability, we anticipate that this reconstruction will have many applications in the study of long-term climate–ecosystem interactions and water resource management. Preliminary comparisons between reconstructed precipitation and existing records of major YNP disturbance events and landscape transitions (Fig. 5) suggest that decadal to multidecadal precipitation variability has been a major force in shaping the region's modern landscapes. This lower frequency variability could significantly alter water yields over 10-yr and longer time scales, with impacts to barge traffic, irrigation, industry and municipal water supplies throughout the Missouri River Basin. We propose that future research should include efforts to identify the mechanisms that link lower frequency precipitation variability to the dynamics of physical and biological systems in this area, as well as exploring how the legacies of long-duration droughts and pluvials persist on the landscape. We also suggest that programs in YNP and other large natural areas designed to detect and mitigate anthropogenic change must place current observations in the context of multidecadal climate variability and the potential for regime-like behavior.

As in all paleoclimatic reconstructions, this record comes with important caveats and limitations. First, in the case of applications in ecosystem science, many important ecological events may be driven by seasonal variations in climate that are not resolved in our annual record. Massive fires during AD 1988 followed extremely dry conditions over the months of July and August, but total annual precipitation for this year was near normal (Fig. 2a). The reconstruction also integrates precipitation over a large and topographically complex region (Fig. 1b), but fine-scale climatic variations can be critical for ecosystem and hydrologic processes on the landscape to watershed scale. Because low-order autocorrelation was removed from the tree ring chronologies used in this reconstruction, the proxy record may not account for many of the physical lags (e.g., ground storage) affecting regional water resources. Finally, while statistical analyses indicate the relative strength of this reconstruction compared to other efforts from the region (e.g., Graumlich et al., 2003; Pederson et al., 2005), it still fails to explain around 45% of the interannual variability in observed precipitation records. This unexplained variance and other limitations of the regression-based reconstruction process (e.g., assumption that the relation between predictors and predictand is stable over time) demand that such proxy records be applied with care.

Conclusions

This tree-ring-based reconstruction provides a statistically robust, well-replicated proxy for precipitation in the Yellowstone National Park region. This record complements existing proxies by integrating precipitation over both the winter months and the growing season. Examination of the long-term record shows that, relative to the previous 700 yr, the early 20th century AD was markedly wet. Extreme wet and dry years during the instrumental period all fall within the range of past variability, and both the duration and magnitude of the worst-case droughts of the 20th century AD (i.e. 1930s and 1950s) were likely equaled or exceeded on numerous occasions in the pre-instrumental era. The reconstruction shows significant decadal to multidecadal variability that can produce strong regime-like behavior in regional precipitation, with the potential for rapid, high-amplitude switching between persistent wet and dry conditions.

When combined with proxy records from other regions, this reconstruction can also be used to examine large-scale patterns of drought and the role of regional to remote forcing in controlling YNP climate. Our preliminary comparisons suggest that YNP droughts and wet periods over multiple time scales are often part of spatially complex, extra-regional to sub-continental precipitation events. Key challenges for future research include linking YNP precipitation variability over decadal to multidecadal time scales to regional physical and ecological processes and separating the impacts of natural climatic regimes from the effects of anthropogenic forcing.

Acknowledgments

Primary funding for this research was provided by National Science Foundation grant #ATM00-82376 to L.J. Graumlich. Additional funding was provided through grants to S.T. Gray from the U.S. Geological Survey, Wyoming Water Development Commission and the University of Wyoming-National Park Service Research Station. D. Muhs, F. Biondi and one anonymous reviewer provided valuable comments and suggestions. M. Pisaric, L. Waggoner, A. Toivola, S. Hill, B. Peters, G. Wolken, R. Eddy and J. King provided field, laboratory and technical assistance.

References

Biondi, F., Waikul, K., 2005. DENDROCLIM2002: a C++ program for statistical calibration of climate signals in tree-ring chronologies. Computers and Geosciences 30, 303–311.

Brown, P.M., Wu, R., 2005. Climate and disturbance forcing of recruitment in a southwestern ponderosa pine landscape. Ecology 86, 3030–3038.

Cayan, D.R., Dettinger, M.D., Diaz, H.F., Graham, N.E., 1998. Decadal variability of precipitation over western North America. Journal of Climate 11, 3148–3166.

Cayan, D.R., Redmond, K.T., Riddle, L.G., 1999. ENSO and hydrologic extremes in the western United States. Journal of Climate 12, 2881–2893.

Cook, E.R., 1985. A time-series analysis approach to tree-ring standardization. Ph.D. Dissertation. University of Arizona, Tucson, Arizona. 171 pp.

Cook, E.R., Woodhouse, C.A., Eakin, C.M., Meko, D.M., Stahle, D.W., 2004. Long-term aridity changes in the western United States. Science 306, 1015–1018.

Dean, J.S., 1994. The medieval warm period on the southern Colorado Plateau. Climatic Change 26, 225–241.

Dettinger, M.D., Cayan, D.R., Diaz, H.F., Meko, D., 1998. North-south precipitation patterns in western North America on interannual-to-decadal time scales. Journal of Climate 11, 3095–3111.

Draper, N.R., Smith, H., 1998. Applied Regression Analysis. Wiley, New York, p. 736.

Enfield, D.B., Mestas-Nuñez, A.M., Trimble, P.J., 2001. The Atlantic multidecadal oscillation and its relation to rainfall and river flows in the continental U.S. Geophysical Research Letters 28, 2077–2080.

Fritts, H.C., 1976. Tree Rings and Climate. Academic Press, London. 567 pp.

Garfin, G.M., Hughes, M.K., 1996. Eastern Oregon Divisional Precipitation and Palmer Drought Severity Index from tree-rings. U.S. Forest Service Intermountain Research Station, PNW, pp. 90–174.

Graumlich, L.J., Pisaric, M.F.J., Waggoner, L.A., Littell, J.S., King, J.C., 2003. Upper Yellowstone river flow and teleconnections with Pacific Basin climate variability during the past three centuries. Climatic Change 59, 245–262.

Gray, S.T., Betancourt, J.L, Fastie, C.L., Jackson, S.T., 2003. Patterns and sources of multidecadal oscillations in drought-sensitive tree-ring records from the central and southern Rocky Mountains. Geophysical Research Letters 10, 1316 (doi:10.1029/2002GL01654).

Gray, S.T., Fastie, C., Jackson, S.T., Betancourt, J.L., 2004a. Tree-ring based reconstructions of precipitation in the Bighorn Basin, Wyoming since AD 1260. Journal of Climate 17, 3855–3865.

Gray, S.T., Graumlich, L.J., Betancourt, J.L., Pederson, G.T., 2004b. A tree-ring based reconstruction of the Atlantic Multidecadal Oscillation since 1567 AD. Geophysical Research Letters 31, L12205 (doi:10.1029/2004GL019932).

Gray, S.T., Betancourt, J.L., Jackson, S.T., Eddy, R.G., 2006. Role of multidecadal climate variability in a range extension of pinyon pine. Ecology 87, 1124–1130.

Haan, C.T., 2002. Statistical Methods in Hydrology, 2nd ed. Iowa State Univ. Press, Ames, Iowa. 378 pp.

Hidalgo, H.G., 2004. Climate precursors of multidecadal drought variability in the western United States. Water Resources Research 40, W12504 (doi:10.1029/2004WR003350).

Holmes, R.L., 1983. Computer-assisted quality control in tree-ring dating and measurement. Tree-Ring Bulletin 43, 69–95.

Jain, S., Hoerling, M., Eischeid, J., 2005. Decreasing reliability and increasing synchroneity of western North American streamflow. Journal of Climate 613–618.

Larsen, E.J., Ripple, W.J., 2003. Aspen age structure in the northern Yellowstone Ecosystem, USA. Forest Ecology and Management 179, 469–482.

Mann, M.E., Lees, J., 1996. Robust estimation of background noise and signal detection in climatic time series. Climatic Change 33, 409–445.

Mann, M.E., Cane, M.A., Zebiak, S.E., Clement, A., 2005. Volcanic and solar forcing of the tropical pacific over the past 1000 years. Journal of Climate 18, 447–456.

Mantua, N.J., Hare, S.R., Zhang, Y., Wallace, J.M., Francis, R.C., 1997. A Pacific interdecadal climate oscillation with impacts on salmon production. Bulletin of the American Meteorological Society 78, 1069–1079.

McCabe, G.J., Dettinger, M.D., 1999. Decadal variations in the strength of ENSO teleconnections with precipitation in the western United States. International Journal of Climatology 19, 1069–1079.

McCabe, G.J., Palecki, M.A., Betancourt, J.L., 2004. Pacific and Atlantic Ocean influences on multidecadal drought frequency in the United States. Proceedings of the National Academy of Sciences 101, 4136–4141.

Meko, D.M., Woodhouse, C.A., 2005. Tree-ring footprint of joint hydrologic drought in Sacramento and Upper Colorado river basins, western USA. Journal of Hydrology 308, 196–213.

Meyer, G.W., Pierce, J.C., 2003. Climatic controls on fire-induced sediment pulses in Yellowstone National Park and central Idaho: a long-term perspective. Forest Ecology and Management 178, 89–104.

NRC (National Research Council), 2002. Ecological Dynamics on Yellowstone's Northern Range. National Academies Press, Washington, D.C. 198 pp.

Pederson, G.T., Gray, S.T., Fagre, D.B., Graumlich, L.J., 2005. Long-duration drought variability and impacts on ecosystem services: a case study from glacier national park, Montana USA. Earth Interactions 10, 1–28.

Romme, W.H., Turner, M.G., Wallace, L.L., Walker, J.S., 1995. Aspen, elk, and fire in northern Yellowstone National Park. Ecology 76, 2097–2106.

Schubert, S.D., Suarez, M.J., Pegion, P.J., Koster, R.D., Bacmeister, J.T., 2004. On the cause of the 1930s dust bowl. Science 303, 1855–1859.

Seager, R., Kushnir, Y., Herweijer, C., Naik, N., Velez, J., 2005. Modeling of tropical forcing of persistent droughts and pluvials over western North America: 1856–2000. J. Climate 4065–4088.

Stahle, D.W., Cook, E.R., Cleavland, M.K., Therrell, M.D., Meko, D.M., Grissino-Mayer, H.D., Watson, E., Luckman, B.H., 2000. Tree-ring data document 16th century megadrought over North America. EOS: Transactions of the American Geophysical Union 81, 121–125.

Sutton, R.T., Hodson, L.R., 2005. Atlantic Ocean forcing of North American and European summer climate. Science 5731, 115–118.

Swetnam, T.W., Betancourt, J.L., 1998. Mesoscale disturbance and ecological response to decadal climatic variability in the American Southwest. Journal of Climate 11, 3128–3147.

Swetnam, T.W., Brown, P.M., 1992. Oldest known conifers in the southwestern United States: temporal and spatial patterns of maximum age. Proceedings of a Workshop on Old-Growth Forests in the Rocky Mountains and Southwest: The Status of our Knowledge, Portal, Arizona, USDA Forest Service General Tech. Rep. RM-GTR213, pp. 24–38.

Weisberg, S., 1985. Applied Linear Regression, 2nd ed., John Wiley, New York. 283 pp.

Whitlock, C., Bartlein, P.J., 1993. Spatial variations of Holocene climatic change in the Yellowstone region. Quaternary Research 39, 231–238.

Wigley, T., Briffa, K., Jones, P.D., 1984. On the average value of correlated time series, with applications in dendroclimatology and hydrometeorology. Journal of Climate and Applied Meteorology 23, 201–213.

Woodhouse, C.A., Overpeck, J.T., 1998. 2000 years of drought variability in the central United States. Bulletin of the American Meteorological Society 79, 2693–2714.

Woodhouse, C.A., Gray, S.T., Meko, D.M., 2006. Updated streamflow reconstructions for the Upper Colorado River Basin. Water Resources Research (in review) 42, W05415 (doi:10.1029/2005WR004455).